Comparison of RIS-Assisted and DF Relay-Assisted NOMA Communication Systems

Jiaqi Li, Seung-Hoon Hwang
Department of Electronics and Electrical Engineering
Dongguk University
Seoul, Korea
kikilee@dgu.ac.kr, shwang@dongguk.edu

Abstract—Reconfigurable intelligent surface (RIS)-assisted non-orthogonal multiple access (NOMA) communication networks represent a current research hotspot. This study presents a comprehensive performance comparison between RIS-assisted and decode-and-forward (DF) relay-assisted NOMA systems in an urban environment. Complete system models are developed for both configurations, and their performance is evaluated across multiple metrics, including transmission power, decoding strategy, number of RIS elements, and energy efficiency under varying data rate requirements. The results reveal that in RIS-assisted systems, the effective user channel quality, and thus the optimal decoding order, can change with the number of RIS elements, requiring dynamic adaptation to maintain fairness and maximise throughput. Furthermore, while the DF relay-assisted system performs better at low to moderate data rates, the RIS-assisted system outperforms it when the data rate exceeds a certain threshold. Notably, as the target data rate increases, the number of RIS elements required to surpass DF relay performance decreases sharply, with only a single RIS element needed when the rate exceeds 8 bit/s/Hz. Although the DF relay-assisted system achieves higher energy efficiency at moderate data rates, the RIS-assisted system becomes the most energy-efficient option in high-rate scenarios, because of its passive design and low perelement power consumption.

Keywords—Reconfigurable intelligent surface (RIS), decodeand-forward (DF) relay, non-orthogonal multiple access (NOMA), beyond 5G (B5G), 6G.

I. INTRODUCTION

Mobile communication systems undergo a generational evolution each decade. Traditional multiple access methods, such as frequency-division multiple access in 1G, timedivision multiple access in 2G, code-division multiple access in 3G, and orthogonal multiple access in 4G, allocate different time-frequency resources to individual users to prevent interuser interference. However, as the global communication network advances toward the beyond 5G (B5G) and even the 6G era, the data rate is expected to reach 1 Tbps, with the latency expected to be less than 1 ms. Non-orthogonal multiple access (NOMA), a technology allowing users to share the same time-frequency resource through varying power levels or superposition coding [1], has emerged as a potential solution to achieve massive connectivity for mobile devices with higher data rates and lower latency in future communication systems.

Additionally, reconfigurable intelligent surface (RIS) frameworks have been established to address the challenges of high-power consumption and poor penetration inherent in high-frequency bands required in B5G and 6G. RISs are equipped with numerous passive reflecting elements that can independently manipulate the amplitude, phase, polarisation, and propagation direction of the incident signal. As illustrated in Fig. 1, a typical RIS consists of three layers, i.e., the antenna

array layer, copper layer, and control circuitry layer [2]. The outer layer, i.e., the antenna array layer, includes a dielectric substrate with numerous reflecting elements, each equipped with several positive-intrinsic-negative (PIN) diodes and field-effect transistors. The ON–OFF status of PIN diodes induces signal phase changes. The middle layer features a copper backplane to prevent signal leakage. Lastly, the control circuitry layer, equipped with the RIS, adjusts the bias voltage to control the ON–OFF status of the PIN diodes.

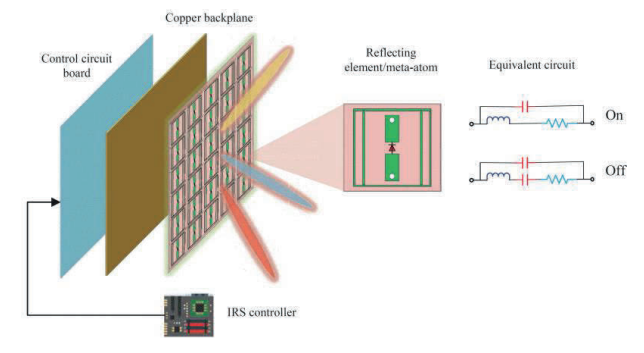


Fig. 1. RIS architecture [2].

Benefiting from the advantages of RIS and NOMA, RISassisted NOMA communication systems have emerged as research hotspots for B5G and 6G applications in recent years [3]. In particular, such systems can maximise the number of served users by providing additional channel paths to construct stronger combined channels with significant strength differences [4]. Additionally, these systems can minimise the total transmission power of the base station and maximise the sum rate by jointly optimising the beamforming of the base station and phase shifts of the RIS. At present, a half-duplex relay plays the same role as the RIS in communication systems, actively processing the received signal before retransmitting the amplified signal. However, the potential performance advantages of RIS-assisted NOMA communication systems over decode-and-forward (DF) relayassisted NOMA communication systems remain to be extensively explored. Therefore, this study is aimed at establishing mathematical methods of RIS-assisted and DF relay-assisted NOMA communication systems and comparing their performances.

II. SYSTEM MODEL

As depicted in Fig. 2, RIS-assisted and DF relay-assisted downlink networks for multiple users are considered in this work, with the DF relay deployed at the same location as the RIS. Notably, NOMA adopts the successive interference cancellation (SIC) technology, which decodes the strongest signal first and then removes the decoded signal from the received signal to eliminate interference from the strongest signal on the weaker signals at the receiver side. In this context,

the decoding order affects the overall system performance, such as the error rate and throughput. However, multiple-input and multiple-output systems are not optimal for NOMA as the relevant channels are not degraded, rendering it challenging to obtain the decoding order [5]. Hence, this work considers a single-input and single-output system in which the base station is equipped with a single antenna to provide services for *K* single-antenna users.

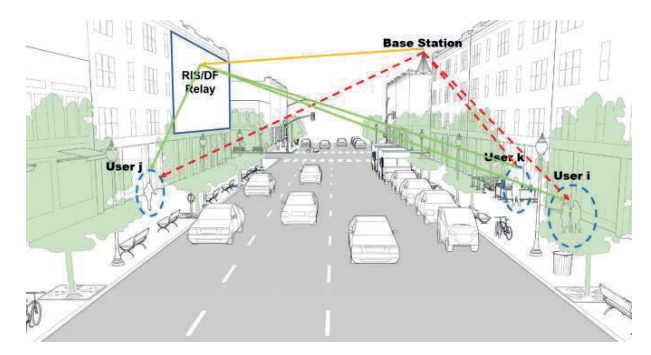


Fig. 2. RIS-assisted and DF relay-assisted multi-user downlink communication systems.

The base station is located at the z-axis with coordinates $(0,0,h_{BS})^{\mathrm{T}}$, establishing a three-dimensional (3D) Cartesian coordinate system. In addition, the locations of the RIS, DF relay, and k^{th} user are defined as $(x_{RIS}, y_{RIS}, h_{RIS})^{\mathrm{T}}$, $(x_{DF}, y_{DF}, h_{DF})^{\mathrm{T}}$, and $(x_{UE,k}, y_{UE,k}, h_{UE,k})^{\mathrm{T}}$, respectively. Specifically, unlike the fixed locations of the base station, RIS and DF relay, users are randomly distributed around the RIS or DF relay within a specific range.

A. Channel Model

The proposed downlink communication, as depicted in Fig. 2, includes three types of channels: the direct channel, incident channel, and reflecting channel. The direct channel (red dotted line), from the base station to the k^{th} user, is denoted by $h_{BS2UE} \in \mathcal{C}$. Considering the presence of obstacles, the direct channels are assumed to be non-line-of-sight (NLOS) channels and modelled using Rayleigh fading [6] as:

$$h_{BS2UE} = \sqrt{PL_0 \left(d_{BS2UE,k}\right)^{-\alpha}} \cdot h_{BS2UE,k}^{NLOS} \tag{1}$$

where PL_0 denotes the path loss at the reference distance, d_{BS2UE} represents the distance between the base station and the k^{th} user, α is the path loss exponent, and $h_{BS2UE,k}^{NLOS}$ represents the NLOS components.

The incident channel (solid yellow line), from the base station to RIS or DF relay, is denoted by $h_{BS2RIS} \in C^N$. Additionally, the reflecting channel (solid green line), from the RIS or DF relay to the k^{th} user, is denoted by $h_{RIS2UE} \in C^N$. Both the incident and reflecting channels are assumed to be line-of-sight (LOS) channels, following Rician fading [9] as the signal received by the user includes the signal that directly reaches the user equipment (UE) in addition to the reflecting and scattering signals from the base station. These channels can thus be defined as:

$$h_{BS2RIS} = \sqrt{PL_0 (d_{BS2RIS})^{-\alpha}} \cdot \left(\sqrt{\frac{\delta}{1+\delta}} \cdot h_{BS2RIS}^{LOS} + \sqrt{\frac{\delta}{1+\delta}} \cdot h_{BS2RIS}^{NLOS} \right)$$
(2)

$$h_{RIS2UE} = \sqrt{PL_0(d_{RIS2UE})^{-\alpha}} \cdot \left(\sqrt{\frac{\vartheta}{1+\vartheta}} \cdot h_{RIS2UE,k}^{LOS} + \sqrt{\frac{\vartheta}{1+\vartheta}} \cdot h_{RIS2UE,k}^{NLOS}\right)$$
(3)

where d_{BS2RIS} is the distance between the base station and RIS or DF relay, and d_{RIS2UE} denotes the distance from the RIS or DF relay to the k^{th} user. h_{BS2RIS}^{LOS} and $h_{RIS2UE,k}^{LOS}$ represent the LOS components of the deterministic channel. h_{BS2RIS}^{NLOS} and $h_{RIS2UE,k}^{NLOS}$ are the NLOS components, characterised as random scattered components. These random variables follow a zero-mean unit variance circularly symmetric complex Gaussian, i.e., $\mathcal{N}_{\mathbb{C}}(0,1)$. The LOS component is the array response of the uniform linear array of RIS, expressed as:

$$h_{BS2RIS}^{LOS} = \left[1, e^{-j\frac{2\pi d}{\lambda}\sin\omega}, \cdots, e^{-j\frac{2\pi d}{\lambda}(N-1)\sin\omega}\right]^{\mathrm{T}}$$
(4)

$$h_{RIS2UE,k}^{LOS} = \left[1, e^{-j\frac{2\pi d}{\lambda}\sin\varphi,k}, \cdots, e^{-j\frac{2\pi d}{\lambda}(N-1)\sin\varphi,k}\right]^{\mathrm{T}}(5)$$

where d denotes the passive reflecting element spacing, λ is the carrier wavelength, N represents the number of RIS elements, and ω is the angle-of-arrival of the incident signal, which can be represented as:

$$\sin \omega = \frac{y_{RIS} - y_{BS}}{\sqrt{(x_{RIS} - x_{BS})^2 + (y_{RIS} - y_{BS})^2}}$$
 (6)

Conversely, φ is the angle-of-departure of the reflecting signal, expressed as:

$$\sin \varphi, k = \frac{y_{UE,k} - y_{BS}}{\sqrt{(x_{UE,k} - x_{BS})^2 + (y_{UE,k} - y_{BS})^2}}$$
(7)

B. RIS-Assisted NOMA-Based System

RIS is assumed to be equipped with N passive reflecting elements, and its diagonal reflection coefficient matrix is defined as:

$$\Theta = \operatorname{diag}(\beta_1 e^{j\theta_1}, \cdots, \beta_N e^{j\theta_N})$$
 (8)

where β denotes the fixed-amplitude reflection coefficient, with $\beta_N \in [0,1]$. θ_n represents the reflecting phase-shift variable for the n^{th} reflecting element, with $\theta_n \in [0,2\pi)$.

Owing to significant path loss, signals that are reflected twice or more by RIS are considered to have negligible intensities. Hence, the signal received by the k^{th} user can be determined by combining the direct signal from the base station and the reflecting signal from the RIS in the RIS-assisted system. In contrast, because the user cluster shares the same time-frequency resources, the signal received by the k^{th} user is a superimposed signal for the NOMA-based system, expressed as:

$$\mathbf{y}_{k} = \left(h_{BS2UE} + h_{BS2RIS}^{\mathrm{T}} \Theta h_{RIS2UE,k}\right) \cdot \sum_{k=1}^{K} \sqrt{\gamma_{k} P_{t}} \cdot s_{k} + n$$
(9)

where P_t denotes the total transmission power, and γ_k signifies the allocated fraction of the total transmission power to the k^{th} user. This allocation is subject to $\sum_{k=1}^K \gamma_k = 1$ and depends on the channel state information. Additionally, s_k denotes the normalised signal for user k, and n represents the additive white Gaussian noise [10] which follows a complex Gaussian distribution with zero-mean and variance of σ^2 , i.e., $n \sim \mathcal{N}_{\Gamma}(0, \sigma^2)$.

According to the Shannon–Hartley theorem, the channel capacity of the k^{th} user in the RIS-assisted NOMA-based communication system is:

$$R(N) = \max_{\theta} \log_2 \left(1 + \frac{\gamma_k P_t \cdot \left| h_{BS2UE} + h_{BS2RIS}^T \Theta h_{RIS2UE} \right|^2}{\sum_{\tau_j > \tau_k} \gamma_j P_j \cdot \left| h_{BS2UE} + h_{BS2RIS}^T \Theta h_{RIS2UE} \right|^2 + \sigma^2} \right)$$
(10)

where τ indicates the decoding order, specifying that user j with higher signal strength should be decoded eariler than user k. This process continues until all users are decoded in the order of decreasing signal strength.

To simplify Eq. (10) the problem of maximizing channel capacity can be converted to that of maximizing the combined channel power gain from the base station to the k^{th} user:

$$\max_{\theta} \left| h_{BS2UE} + h_{BS2RIS}^{\mathrm{T}} \Theta h_{RIS2UE} \right|^{2}, \quad \forall n \in \mathbb{N} \ (11)$$

Accordingly, a triangle inequality can be obtained:

$$\left| h_{BS2UE} + h_{BS2RIS}^{\mathsf{T}} \Theta h_{RIS2UE} \right| \le \left| h_{BS2UE} \right| + \left| h_{BS2RIS}^{\mathsf{T}} \Theta h_{RIS2UE} \right| \tag{12}$$

where the channel model of the incident and reflecting channels is defined as follows:

$$h_{BS2RIS}^{\text{T}}\Theta h_{RIS2UE} = \sum_{n=1}^{N} \beta_n \cdot e^{j\theta n} \cdot [h_{RS2RIS}]_n \{h_{RIS2UE}\}_n [13]$$

The equality of Eq. (13) holds if and only if:

$$\theta_n = \arg\{(h_{BS2UE})\}_n - \arg\{\{h_{BS2RIS}\}_n\{h_{RIS2UE}\}_n\}$$
 (14)

Therefore, Eq. (10) can be rewritten as:

$$R(N) = \log_{2} \left[1 + \frac{\gamma_{k} P_{t'} (|h_{BS2UE}| + \sum_{n=1}^{N} \beta_{n} \beta_{n}|\{h_{BS2RIS}\}_{n} \{h_{RIS2UE}\}_{n}|)^{2}}{\sum_{\tau_{j} > \tau_{k}} \gamma_{j} P_{t'} (\sum_{n=1}^{N} \beta_{n}|\{h_{BS2RIS}\}_{n} \{h_{RIS2UE}\}_{n}|)^{2} + \sigma^{2}} \right]$$
(15)

The energy efficiency can be calculated as:

$$EE_{RIS} = \frac{R_{RIS}}{\frac{P_{t}}{a} + P^{BS} + P^{UE} + N \cdot P^{RIS}}$$
(16)

where e is the efficiency of the power amplifier; P^{BS} , P^{UE} , and P^{RIS} represent the power dissipation of the base station

hardware, UE hardware, and each RIS reflecting element, respectively.

C. DF Relay-Assisted NOMA-Based System

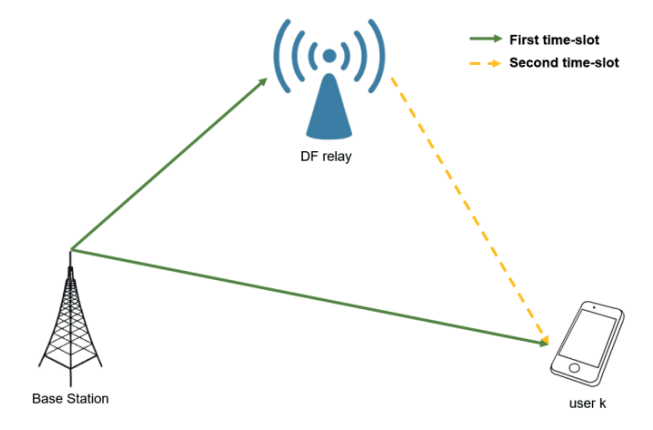


Fig. 3. Conventional half-duplex DF relay transmission.

To reduce the power consumption and enhance reliability, a half-duplex relay, which cannot transmit and receive data simultaneously, is designed to replace RIS and be deployed at the same location as the RIS. Using the classic repetition-coded protocol of the DF relay, signal transmission is performed in two time slots [9], as shown in Fig. 3. In the first time slot, the base station transmits signals to the DF relay and k^{th} user with different transmission power levels. The superimposed transmitted signal can be represented as:

$$x_1 = \sum_{k=1}^K \sqrt{\gamma_k P_t} \cdot s_k \tag{17}$$

The received signal at the DF relay is:

$$y_{BS2DF} = h_{BS2RIS} \cdot x_1 + n_1 \tag{18}$$

The received signal at the k^{th} user is defined as:

$$y_k = h_{BS2UE} \cdot x_1 + n_{2,k} \tag{19}$$

where n_1 and $n_{2,k}$ denote the noise of the DF relay and k^{th} user is defined as:

In the second time slot, the DF relay receives the superimposed signal and decodes it using a specific decoding algorithm. During the decoding process, weaker signals are regarded as noise to prioritise the decoding of the strongest signal. Subsequently, the weaker signal is decoded using the SIC technique, until all signals have been decoded based on their signal intensity. Upon signal decoding, the DF relay reencodes the signal and forwards it to the user. Therefore, the transmitted signal from the DF relay to the k^{th} user can be represented as:

$$x_2 = \sqrt{P_t} \cdot s_k \tag{20}$$

Finally, the signal received by the k^{th} user can be expressed as:

$$y_k = h_{RIS2UE,k} \cdot x_2 + n_{2,k} \tag{21}$$

The channel capacity of the DF relay-assisted NOMAbased communication system is limited by the weakest channel. To ensure a non-negative channel capacity, it is defined as:

$$R_{DF,k} = \max\left\{0, \frac{1}{2}\min\left(R_{BS2UE,k}, R_{BS2DF} + R_{DF2UE,k}\right)\right\}$$
(22)

where $R_{BS2UE,k}$, R_{BS2DF} , and $R_{DF2UE,k}$ denote the capacities of the direct, incident, and reflecting channels, respectively, defined as:

$$R_{BS2UE,k} = \begin{cases} \log_{2} \left(1 + \frac{\gamma_{j} P_{t'} |h_{BS2UE,j}|^{2}}{\gamma_{k} P_{t'} |h_{BS2UE,j}|^{2} + \sigma^{2}} \right), & \text{if } k \neq K \\ \log_{2} \left(1 + \frac{\gamma_{k} P_{t'} |h_{BS2UE,k}|^{2}}{\sigma^{2}} \right), & \text{if } k = K \end{cases}$$
(23)

$$R_{BS2DF} = \log_2 \left(1 + \frac{\gamma_k p_t \cdot |h_{BS2RIS}|^2}{\sigma^2} \right) \tag{24}$$

$$R_{DF2UE,k} = \log_2\left(1 + \frac{P_t |h_{RIS2UE,k}|^2}{\sigma^2}\right)$$
 (25)

The energy efficiency can then be calculated as:

$$EE_{DF} = \frac{R_{DF}}{\frac{P_{f}}{2\rho} + \frac{1}{2} P^{BS} + P^{UE} + P^{DF}}$$
 (26)

III. NUMERIC RESULTS

The aforementioned mathematical models are used to compare RIS-assisted, DF relay-assisted, and non-assisted NOMA downlink systems. Assuming that the coverage range of the base station constitutes a circular area with a radius of 250 m, and to avoid near-field effects, the NOMA user clusters are randomly distributed within the coverage range of 22 m to 250 m. The RIS is assumed to be placed 80 m from the base station on the x-axis [10]. As the RIS reflecting element lacks signal amplification capabilities and the directional gain characteristics of RIS arrays compared with traditional antenna arrays are yet to be defined, a conservative approach is adopted. Specifically, the RIS reflecting element is modelled without directional gain, assuming the maximum gain of a single reflecting element to be 0 dBi [11]. Owing to the decoding complexity associated with SIC technologies, the number of users is set as three. The simulation parameters are summarised in Table I.

TABLE I PARAMETERS

Parameters	Unit	Value
Base station antenna height	m	Urban: 10
Reflecting element gain	dBi	0
Traditional antenna element gain	dBi	8
Carrier frequency	GHz	3.42-3.5
Channel bandwidth	MHz	80
Road width	ft	48
Reflecting element spacing		$0.5\lambda \times 0.5\lambda$
Reflecting element number		100
RIS down-tilt	0	0
RIS height	m	10
UE antenna height	m	1.5
Noise power at the DF relay	dBm	-85
Rician factor	dB	3

Path loss exponent		2.2
Power dissipation of BS, DF relay and UE	mW	100 [9]
Power dissipation of each RIS	mW	5 [9]
Maximum transmission power	dBm	68

A. Relationship between The Number of RIS Elements and User Channel Quality

In the conventional NOMA system, the far user typically experiences poorer channel quality due to increased path loss over long distances, resulting in a lower channel gain compared to the near user. Accordingly, more transmission power is allocated to the far user to maintain fairness and enable effective SIC. However, in the RIS-assisted NOMA system, the overall channel gain can be substantially enhanced by the intelligent reflection of signals from RIS. Notably, as the number of RIS elements increases, the reflected link can significantly improve the effective channel quality, particularly for the far user. When N exceeds a certain threshold, the far user may experience a higher composite channel gain than the near user, thereby reversing the traditional channel ordering assumption in NOMA. To capture this dynamic behaviour, two decoding regimes are defined in this study. Case A refers to the scenario where the near user maintains a stronger effective channel than the far user, consistent with conventional NOMA assumptions. Case B represents the situation where, due to the RIS gain, the far user's effective channel surpasses that of the near user. We analyse the sum rate performance of RIS-assisted NOMA under both decoding strategies across different value of N. As shown in Fig. 4, when N is relatively small, Case A yields a higher sum rate than Case B. The simulation results indicate a crossover point at N = 1556, where both decoding methods achieve an equal sum rate of approximately 9.168. Therefore, for N < 1556, Case A is preferable, whereas for N > 1556, Case B becomes more advantageous.

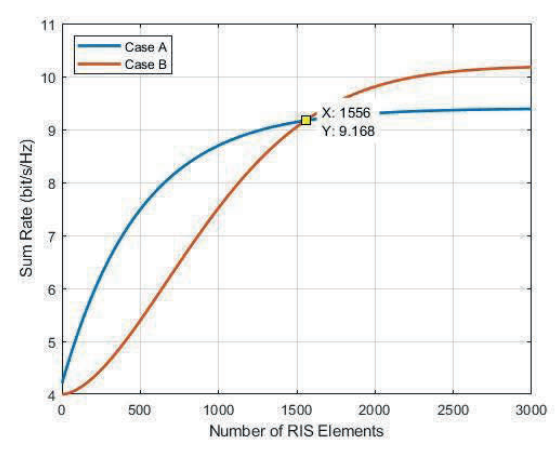


Fig. 4. Sum rate of different decoding methods versus the number of RIS elements.

B. Required Transmission Power

In this analysis, we examine the minimum transmission power required to achieve data rates ranging from 0 to 12 bit/s/Hz, as depicted in Fig. 5. The results indicate that the RIS-assisted system consistently requires less transmission power than the non-assisted baseline. This performance gain is primarily due to the ability of RIS to mitigate the effects of environmental obstructions by intelligently reflecting signals, thereby reducing path loss and signal degradation compared

to direct transmission in the non-assisted system. In contrast, the transmission power required by the DF relay-assisted system increases significantly with the target data rate. Notably, in the urban scenario, its required power surpasses that of the non-assisted system when the data rate exceeds approximately 7.81 bit/s/Hz. This increase is largely attributed to the inherent limitations of half-duplex relaying, where signal decoding and re-encoding at the relay node introduce additional latency and energy cost. As represented by the half pre-log factor in Eq. (22), this constraint effectively reduces spectral efficiency, necessitating a higher signal-tointerference-plus-noise ratio (SINR) to achieve comparable data rates. Furthermore, the RIS-assisted NOMA system begins to outperform the DF relay-assisted system when the target data rate exceeds 6.85 bit/s/Hz, demonstrating the superior power efficiency and scalability of RIS in high-rate communication scenarios, particularly in challenging urban environments.

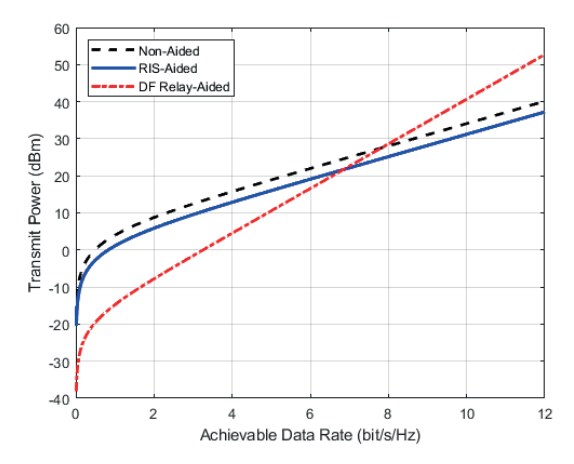


Fig. 5. Transmission power required to achieve different data rates.

C. Number of RIS Elements Required to Surpass DF Relay

In this subsection, we investigate the minimum number of RIS reflecting elements required for the RIS-assisted system to outperform the DF relay-assisted system across various target data rates. The simulation results demonstrate a clear inverse relationship between the required number of RIS reflecting elements and the target data rate. Specifically, at lower data rates, such as 1 bit/s/Hz, a relatively large number of RIS elements, 1168, is necessary to offset the limited spectral efficiency of RIS under low signal strength conditions. As the target data rate increases, the required number of reflecting elements decreases substantially: 872 for 2 bit/s/Hz, 613 for 3 bit/s/Hz, and 406 for 4 bit/s/Hz. This downward trend continues, with only 251 elements needed for 5 bit/s/Hz, 137 for 6 bit/s/Hz, and just 55 for 7 bit/s/Hz. Remarkably, when the target data rate reaches 7.9 bit/s/Hz or higher, a single RIS element suffices for the RIS-assisted system to surpass the performance of the DF relay-assisted counterpart. These findings underscore the superior scalability and spectral efficiency of RIS-assisted systems in high-throughput scenarios. They also highlight the diminishing marginal returns of additional RIS elements in this regime, suggesting that RIS provides a more hardware-efficient solution for highdata-rate applications, whereas achieving competitive performance at lower rates may necessitate a denser RIS deployment.

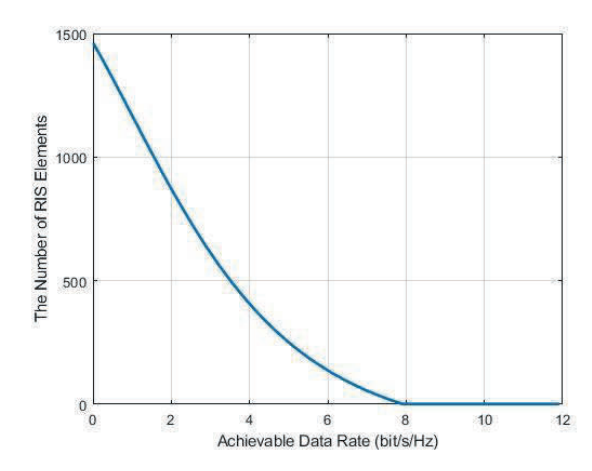


Fig. 6. Minimum number of RIS reflecting elements required for the RIS-assisted system to outperform the DF relay-assisted system.

D. Energy Efficiency

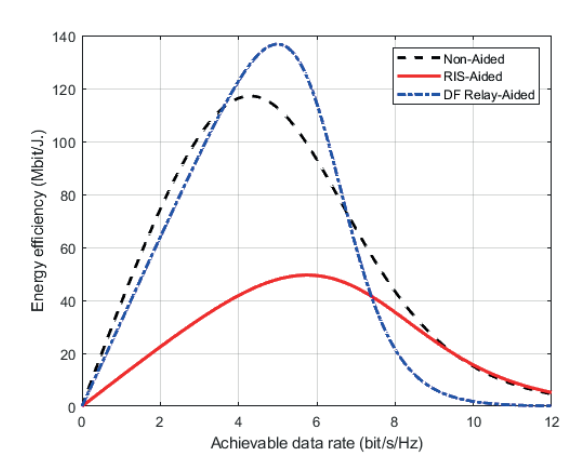


Fig. 7. The energy efficiency versus the achievable data rate.

Fig. 7 shows the energy efficiency as a function of the achievable data rate in the urban scenario. The DF relayassisted system consistently demonstrates higher energy efficiency than the non-assisted system across a broad range of data rates. Specifically, the DF relay-assisted system achieves a peak energy efficiency of approximately 136.75 Mbit/J, compared to 117.15 Mbit/J for the non-assisted system. The DF relay-assisted system outperforms the non-assisted system in the data rate range of 3.62 to 6.75 bit/s/Hz, while the non-assisted system exhibits better energy efficiency at both lower and higher data rate ranges, below 3.62 and above 6.75 bit/s/Hz. In contrast, the RIS-assisted system with 100 reflecting elements shows relatively low energy efficiency across most data rates in the urban scenario. This limitation is primarily due to the fixed and limited passive gain provided by the RIS under low-rate conditions, which is insufficient to compensate for the lack of active amplification. However, the RIS-assisted system demonstrates its strength at high data rates, outperforming both DF relay-assisted and non-assisted systems when the achievable data rate exceeds 9.54 bit/s/Hz. These findings indicate that while RIS-assisted systems may not be energy-efficient at low to moderate data rates, particularly when the number of reflecting elements is constrained, they become more favourable in high-throughput

scenarios. Thus, for applications demanding higher data rates, RIS-assisted communication presents a more energy-efficient alternative, especially in dense urban environments.

IV. CONCLUSION

We formulated a mathematical model to estimate the data rate and energy efficiency of RIS-assisted and DF relayassisted communication systems. Additionally, we compared the decoding order, required transmitted power, number of RIS reflecting elements, and energy efficiency of RIS-assisted, relay-assisted, and non-assisted NOMA-based communication systems. First, we demonstrated that the traditional NOMA user ordering assumption, where the near user has a better channel than the far user, may no longer hold in RIS-assisted systems. As the number of RIS reflecting elements increases, the far user's effective channel gain can exceed that of the near user. We identified a critical threshold, i.e., N = 1556, where the optimal decoding order switches. This highlights the need for dynamic power allocation and decoding strategies based on the instantaneous composite channel conditions in RIS-assisted NOMA. Second, we analysed the required transmission power across a range of target data rates. The RIS-assisted system consistently required lower transmission power than the non-assisted and DF relay-assisted systems, particularly at high data rates. However, due to half-duplex operation and decoding overhead, the DF relay system exhibited higher power requirements as the data rate increased, exceeding the non-assisted baseline at approximately 7.81 bit/s/Hz. Third, we evaluated how many RIS elements are necessary for the RIS-assisted system to outperform the DF relay-assisted system at various data rates. The results revealed an inverse relationship: at low data rates, a larger number of RIS elements is needed, e.g., 1168 for 1 bit/s/Hz, while only a single element is sufficient when the data rate reaches or exceeds 7.9 bit/s/Hz. Finally, our energy efficiency analysis showed that while RIS is inherently lowpower due to its passive architecture, its energy efficiency was lower than that of the DF relay-assisted system at moderate data rates, given the limited gain achievable with only 100 elements. However, the RIS-assisted system outperformed both the DF relay-assisted and non-assisted systems in energy efficiency when the data rate exceeded 9.54 bit/s/Hz, confirming its suitability for high-throughput and energyconstrained applications.

REFERENCES

- [1] Y. Chen et al., "Toward the Standardization of Non-Orthogonal Multiple Access for Next Generation Wireless Networks," in *IEEE Communications Magazine*, vol. 56, no. 3, pp. 19-27, March 2018, doi: 10.1109/MCOM.2018.1700845.
- [2] Q. Wu and R. Zhang, "Towards Smart and Reconfigurable Environment: Intelligent Reflecting Surface Aided Wireless Network," in *IEEE Communications Magazine*, vol. 58, no. 1, pp. 106-112, January 2020, doi: 10.1109/MCOM.001.1900107.
- [3] A. Akbar, S. Jangsher and F. A. Bhatti, "NOMA and 5G Emerging Technologies: A Survey on Issues and Solution Techniques," in *Computer Networks*, vol. 190, p. 107950, ISSN 1389-1286, May 2021, doi: https://doi.org/10.1016/j.comnet.2021.107950.
- [4] G. Yang, X. Xu, Y. C. Liang and M. D. Renzo, "Reconfigurable Intelligent Surface-Assisted Non-Orthogonal Multiple Access," in *IEEE Transactions on Wireless Communications*, vol. 20, no. 5, pp. 3137-3151, May 2021, doi: 10.1109/TWC.2020.3047632.
- [5] S. M. R. Islam, N. Avazov, O. A. Dobre and K. S. Kwak, "Power-Domain Non-Orthogonal Multiple Access (NOMA) in 5G Systems: Potentials and Challenges," in *IEEE Communications Surveys &*

- Tutorials, vol. 19, no. 2, pp. 721-742, October 2017, doi: 10.1109/COMST.2016.2621116.
- [6] B. Zhao, C. Zhang, W. Yi and Y. Liu, "Ergodic Rate Analysis of STAR-RIS Aided NOMA Systems," in *IEEE Communications Letters*, vol. 26, no. 10, pp. 2297-2301, Oct. 2022, doi: 10.1109/LCOMM.2022.3194363.
- [7] Z. Li, W. Chen, Q. Wu, H. Cao, K. Wang and J. Li, "Robust Beamforming Design and Time Allocation for IRS-Assisted Wireless Powered Communication Networks," in *IEEE Transactions on Communications*, vol. 70, no. 4, pp. 2838-2852, April 2022, doi: 10.1109/TCOMM.2022.3152576.
- [8] R. Zhong, Y. Liu, X. Mu, Y. Chen and L. Song, "AI Empowered RIS-Assisted NOMA Networks: Deep Learning or Reinforcement Learning?," in *IEEE Journal on Selected Areas in Communications*, vol. 40, no. 1, pp. 182-196, January 2022, doi: 10.1109/JSAC.2021.3126068.
- [9] E. Björnson, Ö. Özdogan and E. G. Larsson, "Intelligent Reflecting Surface Versus Decode-and-Forward: How Large Surfaces are Needed to Beat Relaying?," in *IEEE Wireless Communications Letters*, vol. 9, no. 2, pp. 244-248, Feb. 2020, doi: 10.1109/LWC.2019.2950624.
- [10] J. Li, S. Liu, and S. -H. Hwang, "A Study on the Optimal Reconfigurable Intelligent Surfaces Placement," 2022 Korean Institute of Communications and Information Science (KICS) Fall Conference, Nov. 2022, Gyeongju, Korea, pp. 541 – 542.
- [11] J. Li, and S. -H. Hwang, "Minimum Required Size of RIS for DF Relay Based on NOMA with Two Users," 2023 Korean Institute of Communications and Information Science (KICS) Winter Conference, Jan. 2023, Pyeongchang, Korea, pp. 162 – 163.